Published online 29 April 2016

Nucleic Acids Research, 2016, Vol. 44, No. 10 ***4855–4870***
doi: 10.1093/nar/gkw346

A putative *Leishmania* DNA polymerase theta protects the parasite against oxidative damage

Abel Fernández-Orgiler[1,†], María I. Martínez-Jiménez[2,†], Ana Alonso[1,†], Pedro J. Alcolea[1], Jose M. Requena[2], María C. Thomas[3], Luis Blanco[2] and Vicente Larraga[1,*]

[1]Centro de Investigaciones Biológicas (CSIC), 28040 Madrid, Spain, [2]Centro de Biología Molecular 'Severo Ochoa' (CSIC-UAM), 28049 Madrid, Spain and [3]Instituto de Parasitología y Biomedicina López-Neyra (CSIC), 18100 Granada, Spain

Received July 21, 2015; Revised April 11, 2016; Accepted April 14, 2016

ABSTRACT

Leishmania infantum **is a protozoan parasite that is phagocytized by human macrophages. The host macrophages kill the parasite by generating oxidative compounds that induce DNA damage. We have identified, purified and biochemically characterized a DNA polymerase θ from** ***L. infantum*** **(*Li*Polθ), demonstrating that it is a DNA-dependent DNA polymerase involved in translesion synthesis of 8oxoG, abasic sites and thymine glycol lesions. Stably transfected** ***L. infantum*** **parasites expressing *Li*Polθ were significantly more resistant to oxidative and interstrand cross-linking agents, e.g. hydrogen peroxide, cisplatin and mitomycin C. Moreover, *Li*Polθ-overexpressing parasites showed an increased infectivity toward its natural macrophage host. Therefore, we propose that *Li*Polθ is a translesion synthesis polymerase involved in parasite DNA damage tolerance, to confer resistance against macrophage aggression.**

INTRODUCTION

Leishmaniasis is a vector borne disease that displays a variety of clinical forms and is caused by various species of the genus *Leishmania* that belong to the trypanosomatidae family (1). It affects nearly 1.5 million low-income populations each year, with a prevalence of 12 million people and an at-risk population of 350 million in 88 countries, most of which are developing countries. In 2013, the W.H.O. declared leishmaniasis to be an emerging disease (2,3). Leishmaniasis clinical form and symptom severity depends on the *Leishmania* species and the host immune status (4). The primary clinical forms of leishmaniasis are cutaneous, mucocutaneous and visceral. Cutaneous leishmaniasis caused by *L. major* and *L. tropica* in the Old World, and *L. infantum* in the Mediterranean basin primarily manifests as self-healing ulcers at the inoculation site. American cutaneous leishmaniasis displays a wider spectrum of clinical manifestations; a hallmark of *L. braziliensis* infection is the mucocutaneous form, which affects the oral and nasal mucosa, causing facial disfiguration and respiratory disturbances in many cases. Visceral leishmaniasis is a severe systemic form of the disease caused by *L. donovani* and *L. infantum* that affects the internal organs, especially the spleen, lymph nodes, liver and guts; untreated, this form is usually mortal (5). In the Mediterranean basin, visceral disease is produced by *L. infantum* (its primary reservoir is the dog) and presents with both cutaneous and visceral symptoms (4). The parasite has a digenetic cycle, taking two forms. The extracellular mobile form, the promastigote, lives in the gut of the sand fly and enters the host through an insect bite. Within the mammalian host, the parasite enters mononuclear phagocyte cells, where it is exposed to an acidic environment, increased temperature, reactive oxygen species (ROS) and other damaging agents. If it survives, the parasite develops into its immobile intracellular form, the amastigote, and proliferates within the cell. Later, the phagocyte explodes and the released parasites infect other mononuclear phagocyte cells. These differentiation processes can be mimicked *in vitro* (6–8).

The recent description of distinct *Leishmania* genome sequences has allowed us to assign known functions to 35% of the protein coding genes (9). One of the inferred genes, Linj24.0910, is overexpressed in the infective parasite (10) and encodes a putative A-family DNA polymerase. Here, we show that this enzyme is nuclear and could represent a *L. infantum* orthologue of DNA polymerase theta (*Li*Polθ).

Several functions have been attributed to Polθ, e.g. repair of interstrand crosslinks, translesion synthesis, base excision repair and double strand breaks repair (11–14). Recently, Polθ was suggested to be involved in the timing of DNA replication (15) as well as in the suppression of genomic instability and genome rearrangements (16). Here, we show that *Li*Polθ is a template-dependent DNA

*To whom correspondence should be addressed. Tel: +34 91 8373112; Fax: +34 91 5360432; Email: vlarraga@cib.csic.es
† These authors contributed equally to this paper as first authors.

polymerase that tolerates oxidative damage, e.g., 8oxoG, thymine glycol and abasic sites. Accordingly, we have observed that *Leishmania* parasites overexpressing *Li*Polθ are more resistant to the oxidative agent hydrogen peroxide and other DNA damaging agents. Moreover, we demonstrate that the rate of infection for *L. infantum* overexpressing *Li*Polθ is 3-fold higher than that of the wild-type strain. As proposed here, *Li*Polθ likely counteracts macrophage antiparasitic activity, resulting in an increased infective capacity and survival.

MATERIALS AND METHODS

Bioinformatics

Family A polymerase amino acid sequences were from the non-redundant protein sequence database at the NCBI. Database search were performed using the Basic Local Alignment Search Tool with default parameters (BLASTP algorithm) (17). Multiple alignments of protein sequences were constructed by COBALT with an *E*-value threshold of 0.003 (18). Multiple-protein-sequence alignments for phylogenetic tree analysis were constructed by CLUSTAL OMEGA using the Neighbor-Joining method (19).

Oligonucleotides

DNA oligonucleotides were synthesized by Sigma Aldrich (St Louis, Mo, USA) and Invitrogen (La Jolla, CA, USA). Oligonucleotides containing 8oxoG were purchased from Eurogentec (Seraig, Belgium). The synthetic AP nucleotide was obtained from LinkTech and used to customize oligonucleotide synthesis. Unlabeled ultrapure dNTPs were supplied by GE (Fairfield, CT, USA). T4 polynucleotide kinase (New England Biolabs, Ipswich, MA, USA) was used for 5′-oligonucleotide labeling with [γ-^{32}P] ATP from Perkin Elmer (Waltham, MA, USA).

*Li*Polθ expression and purification

The *Li*Polθ coding sequence was PCR-amplified using the following primers: 5′-GTAGAATTCCCACCCAAA TCCGCG-3′ and 5′-GATAAGCTTTCAGCCCCCTGTG GGG-3′. The resulting fragment was inserted into a pRSET expression vector containing an N-terminal His-tagged *Li*Polθ fusion protein. *Escherichia coli* BL21(DE3) pLysS cells were transformed with pRSET-*Li*Polθ and grown at 37°C in LB media supplemented with ampicillin (100 μg/ml) and chloramphenicol (35 μg/ml) to an optical density (OD_{595}) of 0.6 before induction with 0.5 mM IPTG for 3 h at 30°C. Cells were then harvested and washed by centrifugation at 4°C with 0.9% NaCl solution. Each gram of pellet was resuspended in 10 ml of lysis buffer (1 M KCl, 60 mM imidazole, 1% Brij 58, 10% glycerol, and 1 mM benzamidine) and stored at −80°C. Suspensions were thawed and centrifuged at 20 000 g for 1 h at 4°C. His-*Li*Polθ remained in the sediment and was resuspended in 3 ml of denaturing buffer containing 3 M GuHCl. The suspension was centrifuged again, and the supernatant was incubated with agarose-IDA-Ni^{2+} for 1 h in batch. The resin was washed with increasing concentrations of imidazole, and His-*Li*Polθ was eluted with 400 mM imidazole and 3 M GuHCl (a summary of the procedure is depicted in Supplementary Figure S1A). The purified protein was analyzed by SDS-PAGE, which indicated that truncated forms were likely obtained in addition to the purified protein (Supplementary Figure S1A). The band corresponding to His-*Li*Polθ was electro-eluted and used for rabbit antibody production using two inoculations with 100 μg each. The specificity of the resulting polyclonal antibody was evaluated by Western blot. The polyclonal antibody did not present any cross-reactivity with *E. coli* proteins and recognized a single band at the expected molecular weight of 125 kDa from total *L. infantum* extracts (Supplementary Figure S1C). Specificity of the antibody for immunofluorescence microscopy (Supplementary Figure S7E and F) was addressed by using an antigen-blocked control serum, obtained by loading 4 ml anti-*Li*Polθ serum into a 4 ml BrCN-activated Sepharose® 4B (Healthcare Europe, Germany) coupled with 2 mg of purified *Li*Polθ (see below) according to the manufacturer instructions.

Cell-free expression of His-*Li*Polθ was achieved using the TNT T7 quick coupled transcription/translation system (Promega, Madison, WI, USA) according to the manufacturer's instructions. *Li*Polθ expression was detected by Western blotting using the polyclonal antibody described above.

To obtain soluble *Li*Polθ protein, the gene was fused to the maltose-binding protein (MBP) C-terminus by PCR amplification using the following primers: 5′-GTAACTAG TATGCCACCCAAATCCGC-3′ and 5′-GATAAGCTTT CAGCCCCCTGTGGGG-3′. *Escherichia coli* BL21 (DE3) pLysS cells were transformed with the pMALC2-*Li*Polθ construct and grown at 37°C in LB media supplemented with ampicillin (100 μg/mL), chloramphenicol (35 μg/ml) and 0.2% glucose until the OD_{595} reached 0.5. To induce overexpression from pMALC2-*Li*Polθ, IPTG was added to a final concentration of 0.3 mM and cells were incubated at 16°C for 2 h. The cells were then harvested and each gram of pellet was resuspended in 10 ml of column buffer (20 mM Tris–HCl (pH 7.4), 200 mM NaCl, and 1 mM EDTA) and stored at −80°C. Cells were thawed and lysed, and cell debris was separated from the soluble lysate by centrifugation. MBP-*Li*Polθ purification was performed using an amylose resin according to standard procedures. Fractions containing MBP-*Li*Polθ were analyzed by Coomassie Blue staining of an 8% SDS-PAGE gel, quantified and stored at −80°C. Purified MBP-*Li*Polθ was detected as a single band of the expected molecular weight, 167 kDa (Supplementary Figure S1B).

DNA polymerase assay using DNA template/primer molecules

DNA polymerase assays were performed using a synthetic DNA template/primer structure. A 5′ [γ-^{32}P]-labeled 15-mer DNA oligonucleotide primer (5′-GATCACAGTG AGTAC-3′) was annealed to a 28-mer DNA oligonucleotide template (5′-AGAAGTGTATCT(**X**)GTACTCAC TGTGATC-3′, where X stands for each dNTP). To produce 1 nt-gapped DNA repair substrates, the template/primer duplex was then annealed to a downstream 12-mer oligonucleotide (5′-AGATACACTTCT-3′). To produce 5 nt-

gapped substrates, the labeled primer was annealed to a 33-mer template (5′-ACTGGCCGTCGTTCTATTGTAC TCACTGTGATC-3′) and a downstream 13-mer oligonucleotide (5′-AACGACGGCCAGT-3′). Assays were performed in a final volume of 20 μl in the presence of 50 mM Tris–HCl (pH 7.5), 1 mM DTT, 50 ng BSA, 2.5 nM labeled DNA, either 1 mM $MgCl_2$ or 100 μM $MnCl_2$, and 200 nM *Li*Polθ. The dNTP concentrations are indicated for each experiment. The reactions were initiated by the addition of labeled DNA and the mixture was incubated at 37°C for 30 min. The negative control lacked protein and dNTPs. The reactions were stopped by the addition of 8 μl of loading buffer (95% formamide, 20 mM EDTA, 0.1% xylene-cyanol, and 0.1% bromophenol blue) and loaded onto 20% polyacrylamide sequencing gels containing 8 M urea. Following denaturing electrophoresis, autoradiography was used to detect primer extension.

Translesion DNA synthesis assays

Substrate containing 8oxoG. Template/primer molecules used for translesion DNA synthesis assays were generated by annealing the 5′ [γ-^{32}P]-labeled 15-mer oligonucleotide to either the control (undamaged) 28-mer oligonucleotide template (5′-AGAAGTGTATCT**G**GTACTCACTGTGATC-3′) or the damaged template in which the G at position 13 (bold) was substituted with 8oxoG. The dNTP concentrations are indicated in the experiment. The reactions were performed and analyzed as described for DNA polymerase assays.

Substrate containing thymine glycol. Primers (5′-GTACCCGGGGATCCGTAC-3′) were 5′ labeled with [γ-^{32}P] ATP and annealed to the undamaged template (5′-CTGCAGCTGATGCGCTGTACGGATCCCCGG GTAC-3′) or the damaged template containing a thymine glycol (X) lesion (5′-CTGCAGCTGATGCGCT**X**GT ACGGATCCCCGGGTAC-3′). The reactions were performed as described above, and the dNTPs concentrations are indicated in the experiment. To evaluate extension of thymine glycol-containing base pairs, the primers (5′-GTACCCGGGGATCCGTACA-3′) and (5′-GTACCCGGGGATCCGTACG-3′) were 5′ [γ-^{32}P]-labeled and annealed to the templates under the same conditions. The reactions were performed and analyzed as described for DNA polymerase assays.

Substrates containing one or more abasic site(s). The DNA substrate was chosen and synthesized according to Seki *et al.* (13). The primer (5′-CACTGACTGTATG-3′) was 5′ [γ-^{32}P]-labeled and annealed to either a control template (5′-CTCGTCAGCATCTTCATCATACAGTC AGTG-3,), a template containing a single abasic site (5′-CTCGTCAGCATCT**X**CATCATACAGTCAGTG-3′; X indicates the position of the tetrahydrofuran molecule) or two abasic sites (5′-CTCGTCAGCATCT**XX**CATCATACAGTCAGTG-3′). The reactions were performed and analyzed as described for DNA polymerase assays.

Parasite strains and culture

L. infantum isolate M/CAN/ES/98/10445 (zymodeme MON-1) was kindly provided by Dr. Alfredo Toraño (Instituto de Salud Carlos III Majadahonda, Spain) and cultured at 27°C in RPMI 1640 supplemented with L-glutamine (Gibco, Waltham, MA, USA), 10% heat inactivated fetal calf serum (Gibco, Waltham, MA, USA), as well as 100 μg/ml streptomycin and 100 IU/ml penicillin (Cambrex, East Rutherford, NJ, USA). *L. major* promastigotes (LV39 line Rho/SU/59/P clone 5) were grown at 27°C in M199 media (Sigma–Aldrich, St Louis, MO, USA) supplemented with 20% heat-inactivated fetal calf serum. Transfected parasites were grown in the presence of 100 μg/ml G418 (Gibco, Waltham, MA, USA).

*Li*Polθ immunolocalization

L. infantum promastigotes were harvested during logarithmic growth by centrifugation at 2000 g for 5 min washed with PBS and resuspended at a concentration of 2 × 10^4 cells/ml in PBS. This suspension (10 μl) was applied to a poly-lysine pre-treated slide and fixed with 4% p-formaldehyde for 5 min at room temperature (RT). The slides were washed three times for 5 min with PBS, incubated with 0.5% Triton X-100 in PBS for 5 min for parasite permeabilization, washed three times again, and blocked with 0.1% Tween 20 + 5% non-fat dry milk in PBS in a wet chamber at 37°C for 30 min. Slides were incubated with rabbit primary polyclonal antibody against *Li*Polθ (diluted 1:50 in blocking solution), with the pre-immune rabbit serum or with the anti-*Li*Polθ serum sequestered with purified *Li*Polθ protein (see above) at RT for 2 h. The slides were then washed three times and incubated in the dark with goat anti-rabbit secondary antibody conjugated to Alexa Fluor 488 diluted 1:200 (Invitrogen) at RT for 1 h. During the last 10 min of incubation, DAPI (diluted 1:2000) was added to the samples. Finally, the slides were washed four times and the samples were mounted in Mowiol. The images were acquired using a (CLSM) Leica TCS SP5 confocal microscope.

Leishmania transfection

The *L. infantum* Polθ coding sequence was PCR-amplified using the following primers: 5′-GTAACTAGTATGCCAC CCAAATCCGC-3′ and 5′-GATAAGCTTTCAGCCCCC TGTGGGG-3′. The resulting fragment was cloned into the pTEX vector (20) between the SpeI and HindIII restriction sites. Parasites were transfected by electroporation according to the high-voltage protocol described by Robinson and Beverley (21). Transfected parasites that stably incorporated the pTEX and pTEX-*Li*Polθ expression vectors were selected by 4 weeks of culturing in the presence of progressively increased G418 concentrations (starting at 5–10 μg/ml and ending at 100 μg/ml).

In vitro macrophage infection

RAW 264.7 macrophages were maintained in RPMI 1640 supplemented with 2 mM L-glutamine, 5 mM $NaHCO_3$ and 10% FCS at 37°C. Cells (0.5 ml for 0.2 × 10^6 cells

per well) were seeded in 24-well plates holding sterilized coverslips, and allowed to adhere for 4 h. Next, non-adherent macrophages were removed and RPMI 1640 media (0.5 ml) with or without metacyclic wild-type, pTEX or pTEX-*Li*Polθ transfected promastigotes (4:1 promastigote:macrophage ratio) was added in triplicate for each experimental point. Metacyclic promastigotes were isolated from the promastigote populations by peanut lectin agglutination (PNA). Briefly, wild-type, pTEX- and pTEX-*Li*Polθ-transfected promastigotes were grown in M199 media supplemented with 20% FCS. After 5 days, stationary promastigotes (2×10^8 cells/ml) were incubated with 50 μg/ml peanut agglutinin (PNA) at RT for 30 min. The supernatants (containing metacyclic promastigotes) were carefully removed by pipetting and centrifuged at 200 g for 10 min. The supernatants were then centrifuged again at 2000 g for 10 min and the metacyclic promastigotes were recovered and resuspended at 1.6×10^6 cells/ml in RPMI 1640 supplemented with 2 mM L-glutamine, 5 mM $NaHCO_3$ and 5% FCS. The plate was incubated at 32°C for 4 h to allow macrophage infection. The media was then retired, any free promastigotes were removed by washing with pre-warmed PBS, 0.5 ml of fresh media was added and the cells were incubated for 72 h. Finally, the media was retired and samples were stained with May-Grünwald-Giemsa. The percentages of infected macrophages were calculated by observing 200 macrophages/well.

Effect of genotoxic agents *in vivo*

Wild-type, pTEX and pTEX-*Li*Polθ-transfected promastigotes were grown in M199 media containing 20% FCS. The parasites were harvested during late exponential growth, washed twice with Hanks buffer (137 mM NaCl, 0.3 mM Na_2HPO_4, 0.4 mM KH_2PO_4, 5.4 mM KCl, and 4.2 mM $NaHCO_3$ (pH 7.2)), resuspended in 0.5 ml of phenol red-free RPMI 1640 media containing 10% FCS and diluted with media to 8×10^6 promastigotes/ml. Dilutions of various genotoxic agents (below) were prepared in phenol red-free RPMI 1640 media supplemented with 10% FCS, and 50 μl were added to 96-well culture plates in triplicate. Wild-type and *Li*Polθ-overexpressing promastigotes were plated at a density of 4×10^6 cells/ml (50 μl/well) and incubated at 27°C for 72 h. Promastigote viability was evaluated using the quantitative colorimetric MTT assay and OD_{595} measurements were obtained using an enzyme-linked immunoabsorbent assay plate reader. In this study, EC_{50} was defined as the concentration that reduced *Leishmania* parasite survival by 50%. The results are expressed as the mean and standard error of three independent experiments. The genotoxic agents and final concentrations evaluated were: 0, 50, 100, 150, 200, 250 and 300 μM hydrogen peroxide (Sigma, St, Mo, USA); 0, 2.5, 5, 10, 25, 50 and 100 μM cisplatin (Sigma-Aldrich); and 0, 0.5, 2.5, 5, 10, 20 and 50 μM mitomycin C (Santa Cruz Biotechnology, Dallas, TX, USA).

RESULTS

A putative *L. infantum* Polθ

The A family of DNA polymerases includes the bacterial PolI, which is involved in DNA repair and Okazaki fragment maturation (22), the mitochondrial replicative polymerase Polγ (23) and the translesion synthesis polymerases Polν and Polθ (13,24). They all share a similar DNA polymerization core (Figure 1A) but differ in their N-terminal domains: Polγ and PolI-like enzymes can possess proofreading 3′-5′ exonuclease domains, whereas Polθ contains an N-terminal helicase domain and a large central domain that is involved in resistance to DNA interstrand crosslinking agents (12).

In silico analysis indicated that the *L. infantum* gene LinJ.24.0910 encodes a putative 1171 amino acid A-family DNA polymerase (125 kDa) that is annotated in several databases as a putative Polθ orthologue. The predicted *Li*Polθ is smaller than the *Drosophila* and *Caenorhabditis* Polθ enzymes, and less than half the size of the human Polθ orthologue (Figure 1A). Accordingly, the predicted *Li*Polθ N-terminal domain lacks any similarity with other eukaryotic Polθ enzymes, and therefore lacks the N-terminal helicase domain that is characteristic of *bona fide* Polθ enzymes. In contrast, *Li*Polθ shares homology with the C-terminal polymerase domain of Polθ, Polν and Polγ that contains the six conserved regions of family A enzymes, including the more universally conserved motifs A, B and C (see Figure 1A). *Li*Polθ is larger than Polν and is similar in size to Polγ, although it lacks the conserved 3′–5′ exonuclease active site (25) that is characteristic of replicative DNA polymerases such as Polγ.

In addition to *Li*Polθ, *L. infantum* possesses four other family A DNA polymerases, which are annotated as mitochondrial PolI-like DNA polymerases as in other trypanosomatids, whose mitochondrial localization have been demonstrated (26). As shown in Figure 1B, these four *Li*PolI (A to D) contain the conserved family A DNA polymerase core, while only *Li*PolIB and *Li*PolID contain the conserved 3′-5′ exonuclease active site as in other trypanosomatids (26–28).

We first performed *in silico* analysis to determine whether *L. infantum* Linj24.0910 encodes a Polθ orthologue. *Li*Polθ exhibited the highest level of amino acid sequence identity with putative orthologues from other members of the subgenus *Leishmania*, e.g. *L. donovani, L. major, L. mexicana* (1) with greater than 90% identity; however, these percentages decreased to 30% when compared with *Trypanosoma* orthologues. Comparisons of the *Li*Polθ C-terminal polymerase domain with metazoan Polθ orthologues and other eukaryotic family A enzymes revealed 25–30% amino acid identity (Supplementary Figure S2). Amino acid sequence alignment revealed that the *Li*Polθ polymerase domain contains the 6 conserved family A DNA polymerization motifs. Moreover, *Li*Polθ presents an insert between the first and second conserved catalytic motifs. Interestingly, this insert (I; brown box in Figure 1A and Supplementary Figure S2) is also conserved in *Homo sapiens* Polθ and is known to be involved in lesion bypass (29).

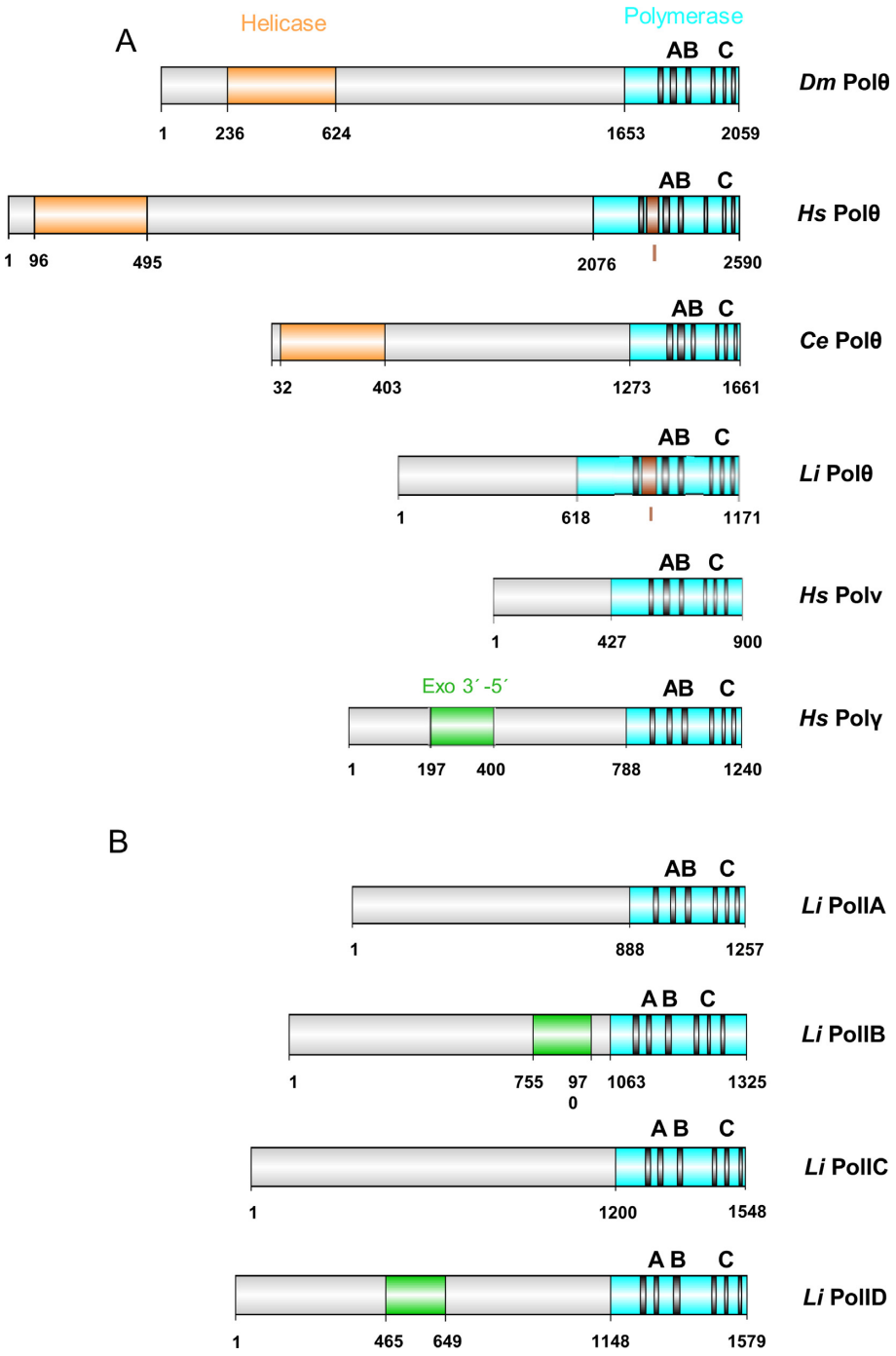

Figure 1. (**A**) Schematic comparison of A-family DNA polymerase sequences from various species. The N-terminal helicase and 3′–5′ exonuclease domains are depicted in orange and green, respectively. The C-terminal DNA polymerase domain is depicted in blue. The grey bars indicate the six conserved regions in family A polymerases, including the A, B and C catalytic motifs. The brown box notes a specific insertion (I) present in *Leishmania infantum* and human Polθ. *Dm*, *Drosophila melanogaster*; *Hs*, *Homo sapiens*; *Ce*, *Caenorhabditis elegans*; *Li*, *Leishmania infantum*. (**B**) Putative mitochondrial *Leishmania infantum* PolI-like DNA polymerases (A, B, C and D).

To establish the evolutionary relationships of LinJ.24.0910 with other polymerases from family A we obtained a phylogenetic tree, strictly using the information of conserved motifs 2/A, 3/B, 5/C, whose extension is defined in Supplementary Figure S2. The resulting tree (Supplementary Figure S3) is divided in two main sub-trees where Polθ and Polν (from metazoan) and putative Polθ (from protozoa) form branches of the same sub-tree (left side in Supplementary Figure S3), whose single root can correlate with a translesion synthesis function; the other sub-tree includes Polγ, Polγ-like and PolI branches that radiate from a single root, that could correlate with their DNA replications tasks (Supplementary Figure S3).

In summary, *in silico* analysis cannot unequivocally clarify if *L. infantum* has a *bona fide* Polθ orthologue but suggests its closer relationship to the Polθ family. Therefore, we decided to characterize the biochemical properties of this putative *Li*Polθ, its cellular localization, and its potential role in DNA damage tolerance, both *in vitro* and *in vivo*.

*Li*Polθ DNA polymerase activity

We tested whether MBP-tagged *Li*Polθ possesses the intrinsic DNA-directed DNA polymerase activity predicted by sequence similarity. Figure 2A shows that *Li*Polθ incorporates deoxynucleotides in the presence of either Mg^{2+} or Mn^{2+} as activating metal ions. Under both conditions, *Li*Polθ could extend the primer strand until the end of the template; however, nearly 100-fold lower dNTP concentrations were required in the presence of Mn^{2+}. These results are consistent with the properties of other *L. infantum* DNA polymerases (30), which exhibited increased activity in the presence of Mn^{2+} ions.

*Li*Polθ fidelity was roughly estimated by providing each nucleotide individually to the four possible templating bases, in the presence of the two alternative activating metals (Mg^{2+} or Mn^{2+}). For a better comparison, we used different dNTP concentrations to allow a similar catalytic efficiency with each alternative metal (see legend to Figure 2B). In both cases *Li*Polθ behaved as a DNA-instructed DNA polymerase, as it preferentially inserted the complementary nucleotide dictated by the first available templating base (Figure 2B). We observed minor +1 bands corresponding to the insertion of non-complementary nucleotides in the case of Mn^{2+}-driven reactions, suggesting that the large improvement in efficiency provided by Mn^{2+} comes at the necessary cost of a reduced nucleotide insertion fidelity. Therefore, we choose Mn^{2+} as a valid metal cofactor for *Li*Polθ.

Figure 2C depicts the polymerization patterns exhibited by purified human Polγ and human PrimPol, for which no template sequence-specific pauses during synthesis were observed. In contrast, purified *Li*Polθ displayed a specific pattern, exhibiting the accumulation of prominent bands following dGMP insertion opposite template C (13), which were also observed when using cell free extracts from *Li*Polθ-overexpressing cells. This signature pattern strongly supports the idea that the polymerase activity observed in the purified fraction is specific and corresponds to a Polθ-like enzyme.

The DNA polymerase activity of *Li*Polθ requires a DNA template. Its inactivity in the absence of template DNA indicates that *Li*Polθ lacks deoxynucleotidyl terminal transferase activity (Supplementary Figure S4, compare panels A and B). *Li*Polθ could partially discriminate incoming nucleotides with or without a 3′-OH, incorporating dGTP 150-fold better than ddGTP (Supplementary Figure S4C). As *L. infantum* is a digenetic parasite having an extracellular form in the vector and an intracellular form in mammalian cells, we assayed *Li*Polθ sensitivity to variations in physiological pH and temperature. As shown in Supplementary Figure S4D, *Li*Polθ DNA polymerase was active between pH 6 and 8, with a maximum activity at pH 7.5. Comparable DNA polymerase activities were observed at temperatures corresponding to the insect vector phase (27°C) and the intracellular phase (37°C).

*Li*Polθ can perform gap-filling coupled to strand-displacement

Processivity is a common feature of DNA polymerases that are involved in extensive DNA synthesis (i.e. replicative polymerases), and relies on tight DNA binding and efficient nucleotide insertion. Conversely, DNA repair polymerases frequently display weaker DNA interactions and distributively incorporate only a few DNA nucleotides on template-primer molecules. DNA repair PolX enzymes such as *Leishmania* Polβ become processive when filling short DNA gaps by specifically recognizing a 5′-phosphate group at the end of the gap (31,32). In contrast with human Polλ, a well-known X family repair polymerase capable of filling 1 nt and 5 nt gaps, *Li*Polθ promoted nucleotide incorporation beyond this gap size limit, and synthesized products that reached the end of the template strand (Figure 3A and B). Moreover, we demonstrated that this gap-filling reaction-associated *Li*Polθ-specific capacity for strand-displacement was not affected by the presence of either a 5′ hydroxyl or a phosphate group in the downstream oligonucleotide flanking the gap (Figure 3C and D). Unlike *L. infantum* Polβ (32) and other DNA repair enzymes, e.g. human Polβ and Polλ, *Li*Polθ is devoid of intrinsic dRP lyase activity (Supplementary Figure S5A and B), demonstrating its inability to participate in short patch base excision repair (BER) (32). In contrast, the efficient strand-displacement of *Li*Polθ (a helicase-like activity) would be invaluable for potential roles in long-patch base excision repair (BER) (33) and alternative non-homologous end-joining processes such as those described for human Polθ (34,35).

*Li*Polθ tolerates oxidative DNA lesions

*Li*Polθ displays DNA polymerization activity and lacks both proofreading exonuclease and dRP-lyase activities, suggesting that *Li*Polθ may act in translesion synthesis (TLS) to facilitate elongation across a damaged template. Human Polθ was previously shown to perform translesion DNA synthesis (TLS) beyond AP sites and thymine glycol adducts (13). We tested whether *Li*Polθ could tolerate the most common oxidative lesion found in DNA: 8 oxo-7, 8 dihydro-2′-deoxyguanine (8oxodG) (36). This damage can result from direct oxidation of deoxyguanine and from primary oxidation of free dGTP that is then incorporated to the DNA double helix (37). 8oxodG is highly premutagenic, and gives rise to dG:dC to dT:dA transversions (38).

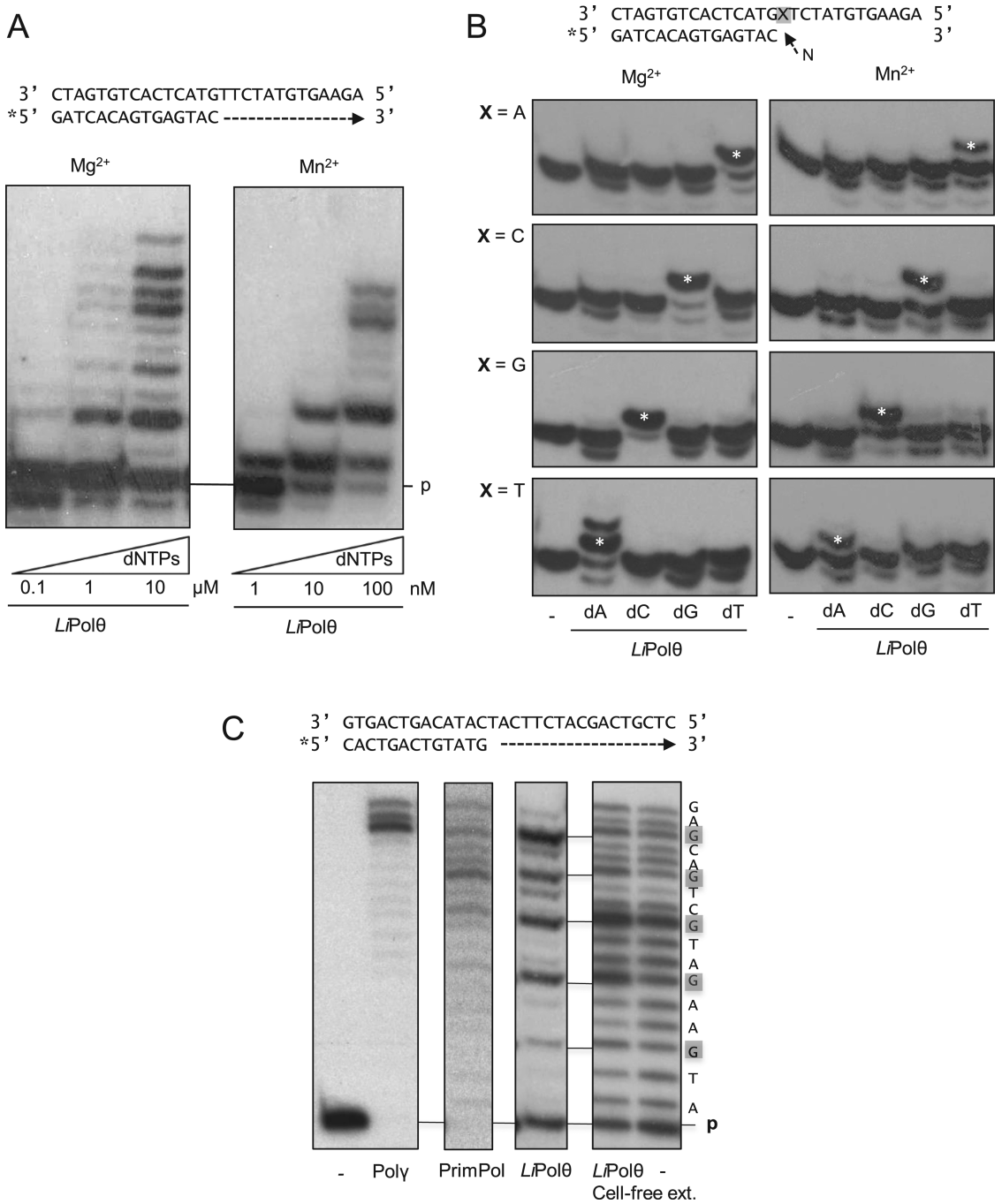

Figure 2. *Li*Polθ possesses intrinsic DNA-directed DNA polymerase activity. (**A**) DNA polymerase activities of *Li*Polθ (200 nM) toward the indicated template/primer structures were evaluated using increasing dNTP concentrations in the presence of either 1 mM $MgCl_2$ (left) or 0.1 mM $MnCl_2$ (right) metal cofactors. Some nucleolytic degradation of the original primer, mainly occurring at low dNTP concentrations, indicates the existence of some contaminant nuclease. (**B**) Four template/primer structures (2.5 nM), differing in the first template base (X), were used for analysis of *Li*Polθ (200 nM) complementary nucleotide. Nucleotide concentrations were 100 nM in the presence of Mg^{2+}, and 1 nM in the presence of Mn^{2+}. Asterisk indicates the main extension of the primers in each panel. (**C**) *Li*Polθ DNA polymerase 'signature'. From left to right: negative control (no enzyme); human Polγ (20 nM); human PrimPol (200 nM); purified *Li*Polθ (200 nM); cell-free extract expressing *Li*Polθ (5 μl); and cell free control extract (5 μl).

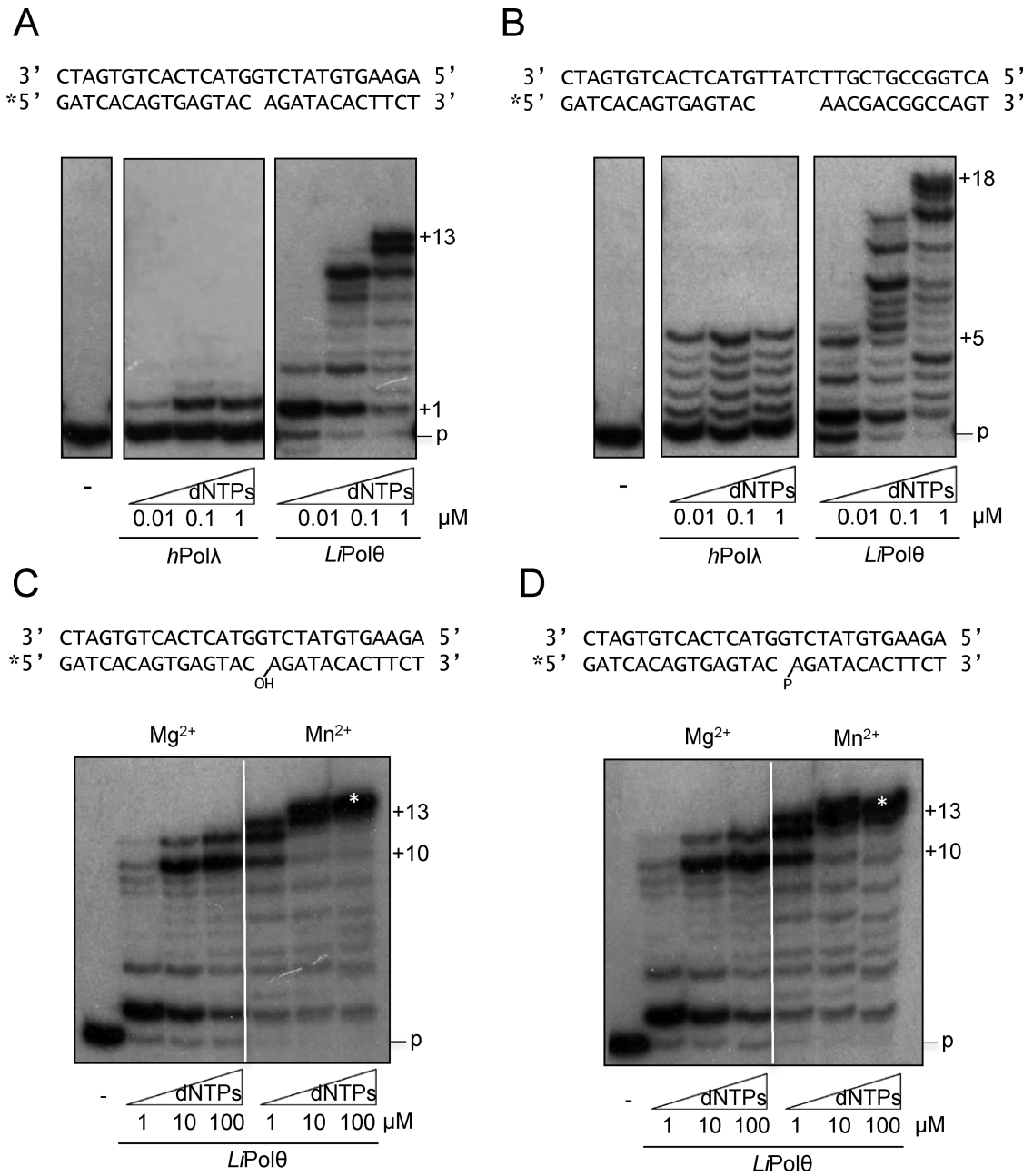

Figure 3. *Li*Polθ can fill gaps and perform strand-displacement. (**A**) Gap1/P: 1-nucleotide gap and (**B**) Gap 5/P: 5-nucleotides gap flanked by a 5′-phosphate. Human Polλ and *Li*Polθ (200 nM) were incubated with the indicated DNA substrates (2.5 nM) and either 1 mM or 0.1 mM $MnCl_2$ (Polλ and *Li*Polθ, respectively), and increasing dNTP concentrations (0.01–1 μM). (**C**) Gap1/OH and (**D**) Gap1/P, 1-nucleotide gaps with either flanking 5′ hydroxyls or phosphates, were incubated with 200 nM *Li*Polθ in the presence of 1 mM $MgCl_2$ or 0.1 mM $MnCl_2$, respectively. Asterisk indicates an extra nucleotide addition in the presence of Mn^{2+} and high dNTP concentration.

As shown in Figure 4A, *Li*Polθ efficiently performed TLS in the presence of Mn^{2+} and the 4 dNTPs by inserting a nucleotide opposite the 8oxodG lesion and catalyzing its further extension to a full size product (14-mer). As 8oxodG can base pair with either cytosine or adenine (the latter generating G to T transversions) we also quantified *Li*Polθ accuracy when copying 8oxodG by measuring the dC:dA ratio. *Li*Polθ preferentially incorporated dCTP opposite an undamaged G by a factor of approximately 10^5 (Mg^{2+}) and 10^2 (Mn^{2+}) (Figure 4B). In contrast, the fidelity ratio (dCTP:dATP) was significantly reduced when copying 8oxodG, to approximately 10^3 and 30 in the presence of Mg^{2+} and Mn^{2+}, respectively (Figure 4B), in both cases still favoring an error-free bypass. These measurements were made at low nucleotide concentrations within the nanomolar range measured in macrophages (Supplementary Figure S6). Undamaged pairs were 10-fold better extended compared with the damaged pairs (8oxodG:dC and 8oxodG:dA). *Li*Polθ more efficiently and accurately extended 8oxodG:dC pairs compared with 8oxodG:dA pairs (Figure 4C); in the latter

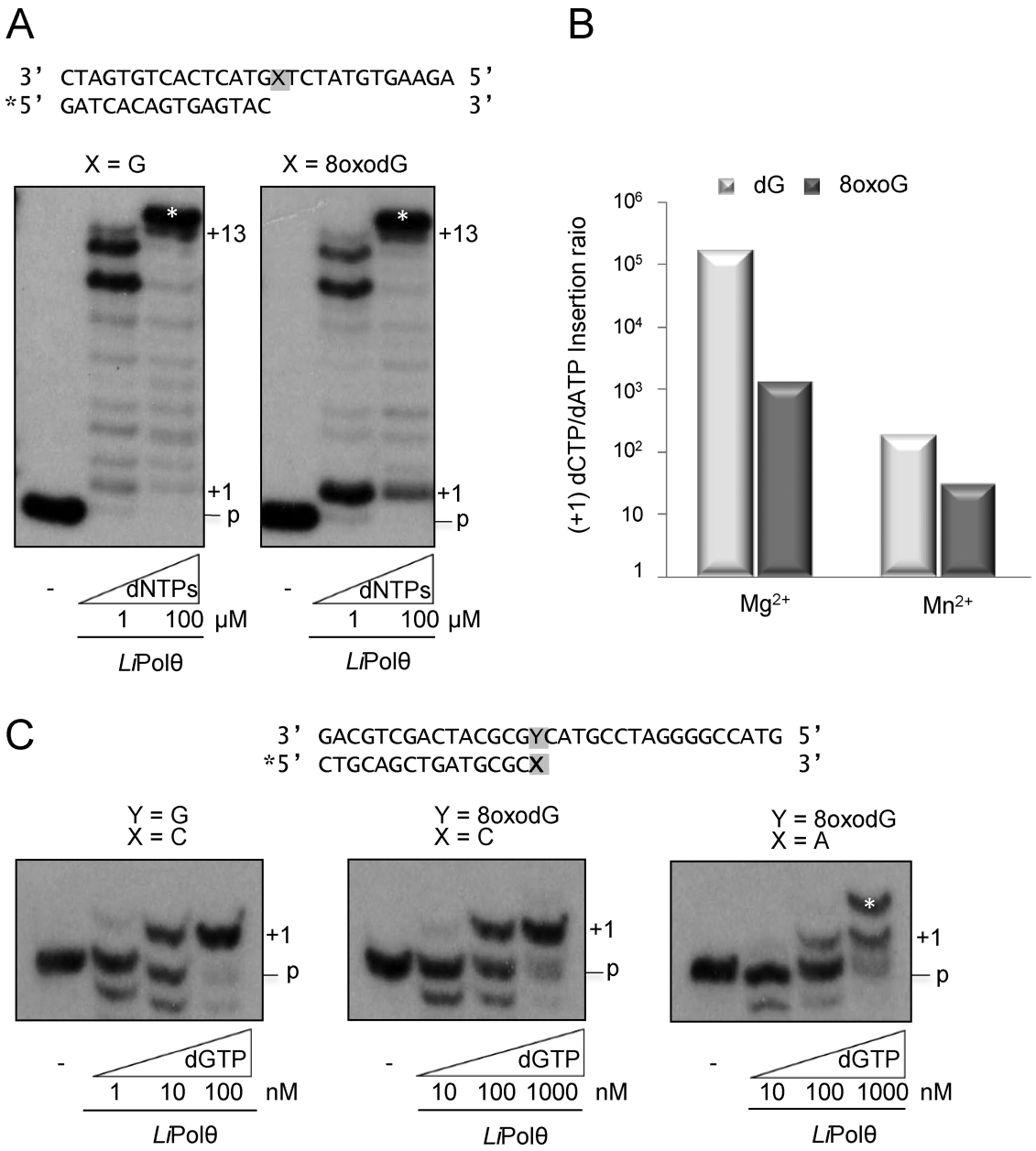

Figure 4. *Li*Polθ bypasses 8oxodG. (**A**) *Li*Polθ DNA polymerization on undamaged template (left) and template containing a 8oxodG lesion (right) in the presence of 200 nM *Li*Polθ, 0.1 mM Mn^{2+}, and the indicated dNTP concentrations. (**B**) Quantification of the insertion ratio (dC versus dA) opposite a control G or an 8oxoG lesion in the presence of either 1 mM $MgCl_2$ or 0.1 mM $MnCl_2$ (derived from the experiment shown in Supplementary Figure S6) (**C**) *Li*Polθ extension of matched (dG:dC or 8oxodG:dC) and mismatched (8oxodG:dA) pairs in the presence of increasing concentrations of the next complementary nucleotide (dGTP).

case, we observed misincorporation of an extra dA (Figure 4C and Supplementary Figure S6C).

Another common DNA lesion is oxidation of thymine to form thymine glycol (Tg), which blocks the replication fork. There are two alternative pathways for Tg bypass: (i) DNA polymerases κ and ζ can act together to mediate error-free TLS (39); and (ii) Polθ can function in an error-prone manner as recently proposed in human cells (40). To evaluate the competence of *Li*Polθ to bypass Tg lesions, we used template/primer structures in which the first template base was either T or Tg, and Mn^{2+} as the preferred metal activator. As shown in Figure 5A, *Li*Polθ is apparently capable of 'reading' the Tg lesion; however, only a fraction of the resulting +1 product was elongated and reached a size that was 1-nt shorter than that obtained with the undamaged template control, suggesting that efficient Tg bypass requires lesion skipping. Analysis of the first insertion event opposite Tg (Figure 5B) showed that in addition to dATP (likely directed by the Tg lesion), *Li*Polθ can insert dGTP (likely directed by the adjacent 5′ dC in the template). To assess the possibility that the observed +15 extension may result from an initial Tg skipping event (inserting dG op-

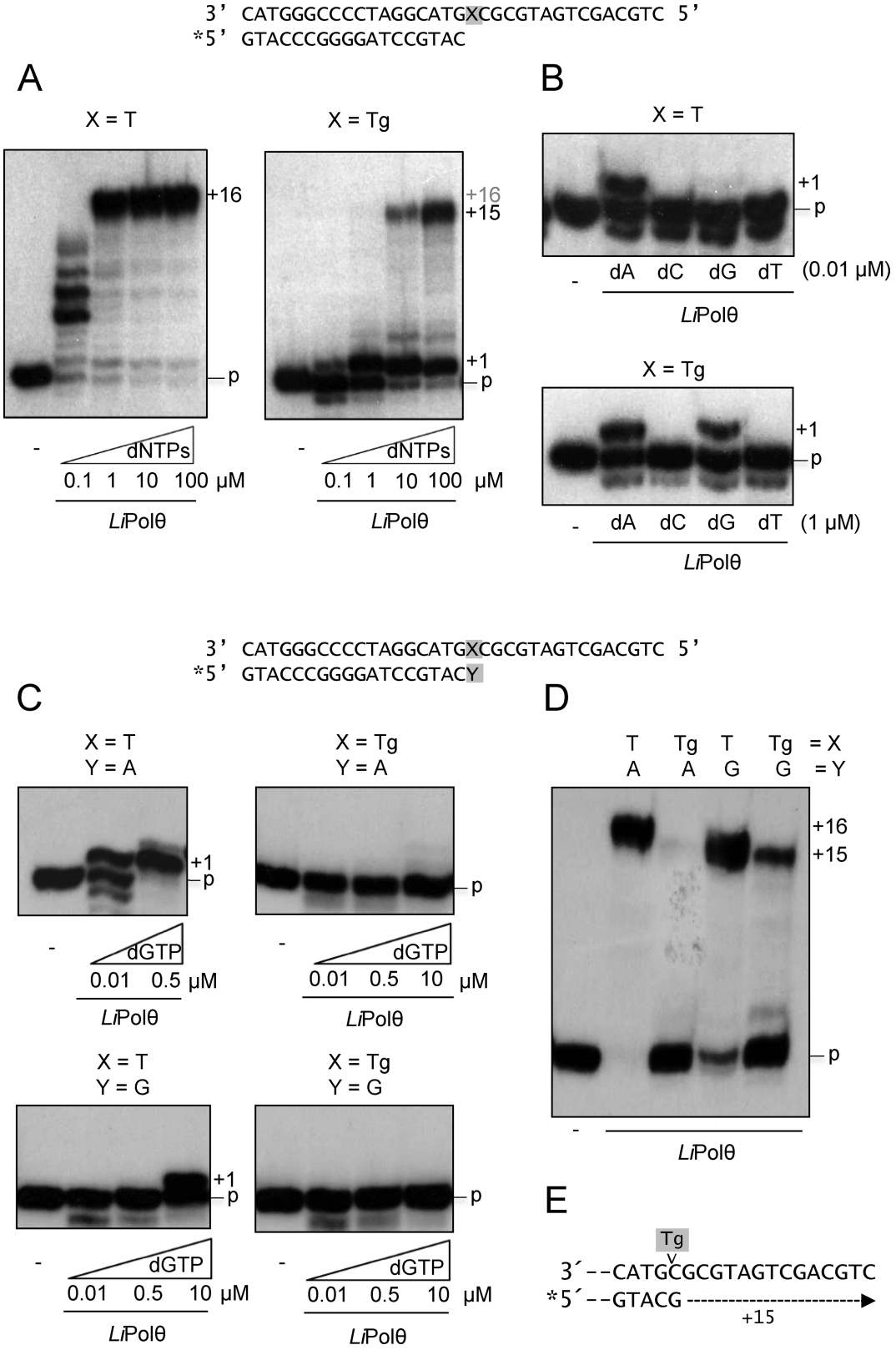

Figure 5. *Li*Polθ tolerates thymine glycol lesions. (**A**) *Li*Polθ DNA polymerase activity on undamaged (left, X = T) and thymine glycol lesion-containing (right, X = Tg) templates, assayed with increasing dNTP concentrations (0.1, 1, 10 and 100 μM). Full extension of the primer has been indicated (+16 in the control template or +15 in the damaged template; the position of a putatrive +16 product is also indicated (in light gray) for the damaged template. (**B**) Assay of nucleotide selectivity of *Li*Polθ reading a control base (T), or a thymine glycol-containing template in the presence of the indicated concentrations of individual nucleotides. (**C**) *Li*Polθ extension of matched (dT:dA and Tg:dA) and mismatched (dT:dG and Tg:dG) in the presence of the indicated

posite the neighbor dC template) additional experiments were performed using DNA substrates containing either the preformed base pairs Tg:dA and Tg:dG, or the corresponding non-damaged dT:dA and dT:dG controls. When dGTP (complementary to the first template base) was provided, *Li*Polθ extended the control pairs dT:dA and dT:dG (Figure 5C, left panel); however, Tg:dA and Tg:dG pairs were inefficiently extended (Figure 5C, right panel). In contrast, when all four dNTPs were provided (Figure 5D), the Tg:dA pairs were very poorly extended, while both dT:dG and Tg:dG mispairs were extended through the +15 position. This product was 1 nt shorter than that observed for the control dT:dA, suggesting that the Tg lesion is looped-out and the 3′-terminal G is paired with the next template base C (see the scheme in Figure 5E). In conclusion, *Li*Polθ can insert dA opposite Tg; however, additional elongation cannot occur through direct extension, but rather requires a Tg-skipping event based on primer-realignment beyond the lesion. It is possible that after *Li*Polθ has introduced dA opposite the damage, a DNA polymerase switch occurs to allow error-free bypass.

Under physiological conditions, abasic sites are the most common DNA chain lesions that result from DNA glycosidase activity and oxidative stress-induced spontaneous hydrolysis of the N-glycosidic link between the sugar and the DNA base (41). Abasic sites block replicative DNA polymerases and the lack of coding information induces mutagenesis (42). Similar to other polymerases, human Polθ preferentially inserts adenine at these abasic sites (13). We tested the capacity of *Li*Polθ to bypass this lesion in the presence of either one or two abasic sites in the template DNA using Mn^{2+} as the preferred metal activator. Figure 6A demonstrates that *Li*Polθ partially pauses immediately before the abasic site (+3); however, approximately 50% of the primers were extended in the presence of moderate concentrations of dNTPs (10 μM). Regardless, the resulting product was one nucleotide shorter than the control when copying the two damaged templates (Figure 6A). When the elongation patterns were compared, it became obvious that either one or two consecutive abasic sites were skipped (Figure 6B; see legend for further details). Insertion of the individual nucleotides was tested using four different DNA sequence contexts in which the nucleotide immediately 5′ of the abasic site was altered (Figure 6C). We evaluated whether *Li*Polθ dislocated the template by nucleotide selection. We did not observe insertion of a pyrimidine (either dC or dT) in any context, even when the template base following the abasic site was a purine (Figure 6C, first and third panels). This observation implies that *Li*Polθ cannot always loop-out the abasic site to copy the next available base; however, both purines were inserted in each context. Insertion of dA likely occurs opposite the abasic site, as it can be extended using a second dA when the next template base is dT (Figure 6C, fourth panel). *Li*Polθ could also insert dG opposite the abasic site, and opposite the second template base in the most favorable contexts, forming either a dC:dG pair or a dT:dG 'pseudopair' (Figure 6C, second and fourth panels). Therefore, *Li*Polθ preferentially incorporates either a dA or a dG opposite to abasic sites but cannot extend it, as we ultimately observed a +1 product. It is possible that another polymerase takes over elongation following *Li*Polθ insertion of a purine in front of the abasic site.

*Li*Polθ is localized in the nucleus and its overexpression does not affect cell growth

*Li*Polθ was initially isolated from an *L. infantum* library clone (10), PCR-amplified, cloned into a pRSET plasmid and purified with an agarose-Ni^{2+} column as described in the materials and methods. The purified protein was used to generate a specific polyclonal antibody that produced a single band by Western blot analysis of whole *L. infantum* extracts in contrast with the control serum and was not significantly cross-reactive with *E. coli* proteins (Supplementary Figure S1C). This antibody was used to immunolocalize *Li*Polθ within the parasite. As shown in Figure 7, *Li*Polθ was colocalized with DAPI staining, indicating a primarily nuclear localization, with a minor presence in the second DNA-containing compartment, the kinetoplast, which contains the mitochondrial DNA and the RNA editing minicircles. This distribution and the specific features described above support the idea that *Li*Polθ is primarily involved in translesion synthesis during nuclear DNA replication.

As in the subgenus *Leishmania Leishmania* RNA interference technology is not affordable, the effect of reduction/loss of *Li*Polθ can not be easily measured. Thus, we studied the effect of over-expression of the enzyme on the parasite behavior. Due to their high genetic similarity, *L. major* and *L. infantum* promastigotes were transfected with a *Li*Polθ (pTEX-*Li*Polθ) and empty expression vectors (pTEX). Transfectants were selected with geneticin as described in the materials and methods, and *Li*Polθ overexpression was verified by Western blotting of promastigote protein extracts (Figure 8A). The transfected *L. major* parasites displayed increased geneticin resistance compared with *L. infantum* parasites (data not shown) and expressed greater amounts of the enzyme. Interestingly, the growth curves of *Li*Polθ-overexpressing *L. major* parasites were similar to those of the *L. major* wild-type (Figure 8B). Consequently, we evaluated the resistance of *Li*Polθ-overexpressing *L. major* parasites to several genotoxic agents *in vivo*.

*Li*Polθ overexpression reduces the effects of genotoxicants and improves infectivity

Once into the mammalian host, *Leishmania* parasites enter the phagocyte cells where they must then resist macrophage activity, which is primarily exerted through an oxidative burst. Using *in vitro* studies, we have demonstrated that purified *Li*Polθ can tolerate various oxidative lesions in DNA;

←

concentrations of the next complementary nucleotide (dGTP). (**D**) *Li*Polθ extension of matched (dT:dA and Tg:dA) and mismatched (dT:dG and Tg:dG) in the presence of all four nucleotides (100 μM). The experiments were performed as described in the materials and methods using 2.5 nM labeled DNA, 200 nM *Li*Polθ and 0.1 mM $MnCl_2$. (**E**) Schematic of the primer extension (+15) observed in part D with template containing the Tg:dG mismatched pair.

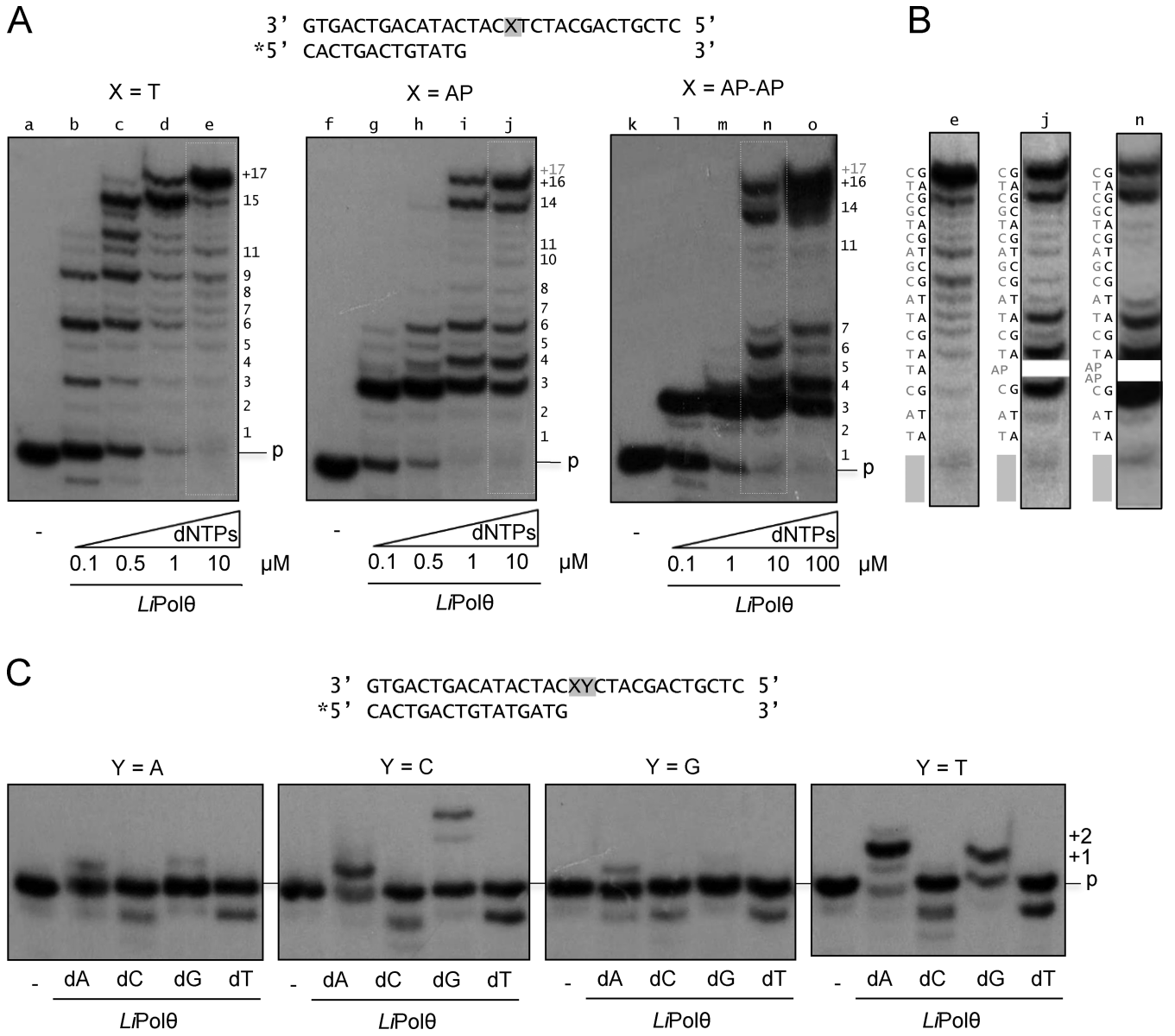

Figure 6. *Li*Polθ skips template abasic sites. (**A**) *Li*Polθ 'running start' polymerase assays on either control (left panel, X = T) or damaged templates containing one (central panel, X = AP) or two (right panel, X = AP-AP) abasic sites, assayed with the indicated dNTP concentration (0.1, 1, 10, 100 μM). Note that the oligonucleotide containing the two abasic sites is 1 nt longer (31 mer) than the other two oligonucleotides (30 mer; control and 1 abasic site). (**B**) Lanes e, j and n from part A, now indicating the template sequence (in gray) and primer extended products (in black) aligned with each corresponding band. A discontinuity in the autoradiograms of lanes j and n has been artificially made to visualize the recovery of the same band pattern beyond the +4 control product. That implies the skip of one or two abasic sites in lanes j and n, respectively. (**C**) *Li*Polθ insertion of each individual nucleotide (10 μM) opposite an abasic site (X), followed by the various nucleotides (Y). The experiments were performed as described in the materials and methods using 2.5 nM labeled DNA, 200 nM *Li*Polθ and 100 μM $MnCl_2$.

consequently, we measured *Li*Polθ-overexpressing parasite resistance to an oxidative reagent, H_2O_2. This analysis indicated that transfected parasites had ∼40% greater resistance (measured as EC_{50}, Table 1) compared with the wild-type strain and pTEX control. We also evaluated the possible role of *Li*Polθ in tolerance to other toxic agents that would affect parasite viability. The inhibitory effects of mitomycin C and cisplatin (DNA interstrand crosslinks) were clearly reduced in the *Li*Polθ-overexpressing parasites compared with the wild-type and control: the cisplatin EC_{50} was increased two-fold and the mitomycin C EC_{50} was increased 6-fold (Table 1).

Wondering whether the levels of *Li*Polθ overexpression affected parasite behavior during infection, the infectivity of transfected and wild-type parasites was measured. As shown in Figure 8C, *Li*Polθ-overexpressing parasites infected RAW macrophages 3-fold more efficiently compared with the wild-type strain and parasites transfected with empty plasmid. This increase in infectivity can be explained by a role of *Li*Polθ in parasite tolerance to oxidative damage due to macrophage attack.

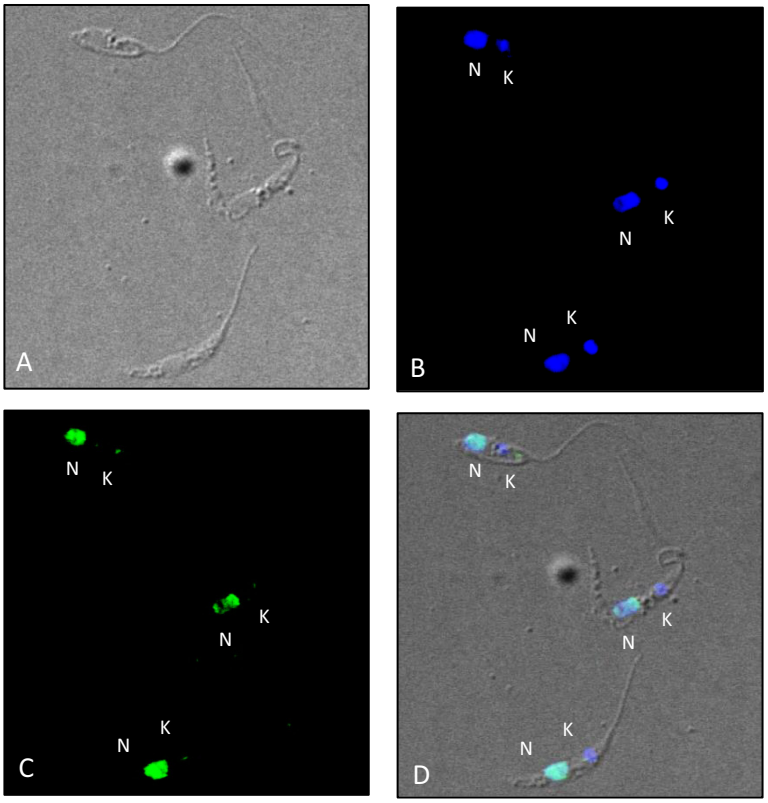

Figure 7. Immunofluoresence indicates that *Li*Polθ is primarily localized in the nucleus.*Leishmania* specimens incubated with anti *Li*Polθ-specific antibody: (**A**) phase contrast; (**B**) DAPI staining; (**C**) *Li*Polθ fluorescence staining with anti *Li*Polθ antiserum; (**D**) merged image of fluorescence and DAPI staining of *Leishmania* specimens. N: nucleus. K: kinetoplast. See Supplementary Figure S7 for controls.

Table 1. Genotoxic damage of control and LiPolθ-overexpressing L. major strains

Agent, damage type	*L. major* WT (EC_{50})	*L. major* pTEX (EC_{50})	*L. major* pTEX-*Li*Polθ (EC_{50})
H_2O_2, oxidative	95 ± 4 μM	92 ± 5 μM	155 ± 3 μM
Cisplatin, ICL	50 ± 3 μM	57 ± 4 μM	99 ± 5 μM
Mitomycin C, ICL	4 ± 1 μM	6 ± 1 μM	26 ± 2 μM

ICL: Interstrand crosslinks.

Together, these *in vivo* data are fully compatible with the *in vitro* results described in this paper, suggesting that *Li*Polθ functions directly in parasite viability by contributing to tolerance of macrophage-inflicted oxidative damage.

DISCUSSION

Polθ, an A family TLS polymerase, is found in protists, plants and animals; however, the structural differences found between these enzymes has led to several authors to be hesitant to suggest whether the species described thus far possess true Polθ orthologues (13). As annotated in several public databases, the *L. infantum* gene LinJ.24.0910 encodes a putative Polθ orthologue (*Li*Polθ), although it differs from other *bona fide* Polθ in that the N-terminal helicase domain is absent. As demonstrated here, detailed evaluation of the amino acid sequence identities of the six more highly conserved segments/motifs in the C-terminal polymerase domain shared by all family A DNA polymerases (including the eukaryotic Polθ, Polν, Polγ and PolI-like enzymes) did not clarify whether *Li*Polθ is indeed a Polθ orthologue. In contrast, homology is suggested by phylogenetic tree analysis using these conserved DNA polymerase motifs, in which *Li*Polθ similarly roots with two other family A subgroup members, the TLS polymerases Polθ and Polν.

Recombinant *Li*Polθ was fused to MBP and expressed in *E. coli*, favoring protein solubility, purification and stability. Biochemical characterization of *Li*Polθ indicated that it is a DNA-dependent DNA polymerase displaying basic features that correspond to diverse family A members (11). *Li*Polθ activity is highest at pH 7.5, although it remains active in moderately acidic environments (pH 6), matching the environment within the macrophage. *Li*Polθ is active within a temperature range of 27–37°C, which are found in the vector and host, respectively. As anticipated from the lack of *bona fide* Exo motifs (25), *Li*Polθ is devoid of 3′-5′ proofreading exonuclease activity, in contrast with eukaryotic Polγ and two family A DNA polymerases present in *Leishmania* (*Li*PolIB and *Li*PolID), that have been shown to be proofreading-competent in their *Trypanosome* orthologues (26–28). *Li*Polθ also lacks terminal transferase ac-

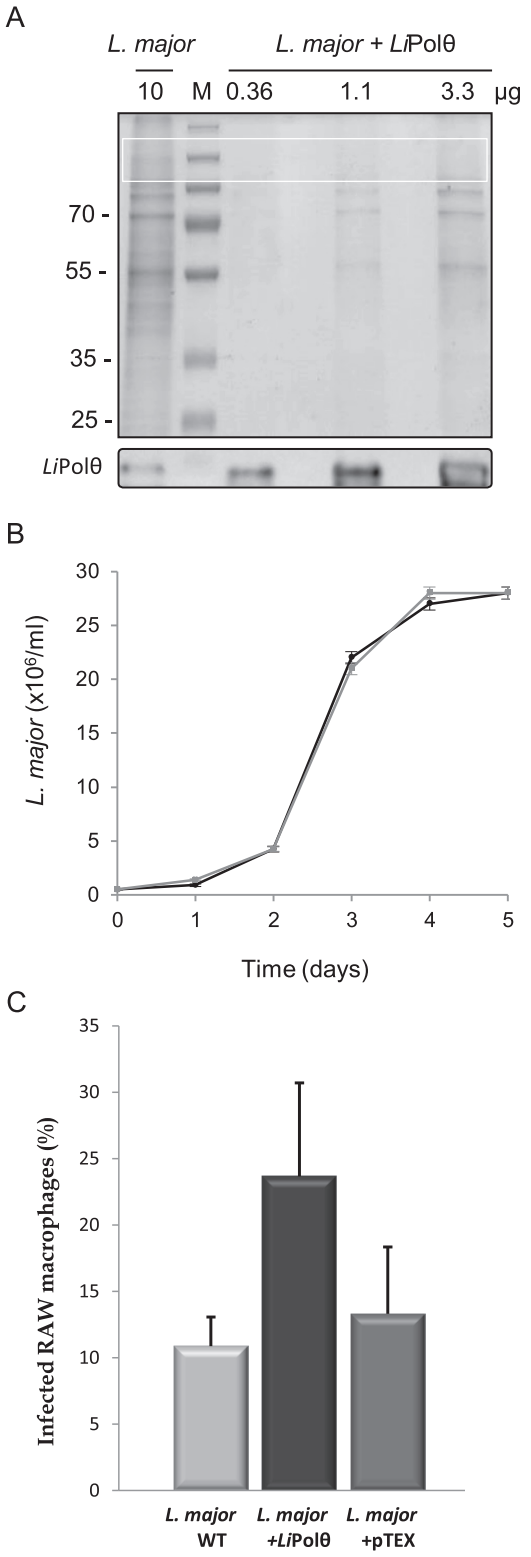

Figure 8. *Li*Polθ overexpressing *Leishmania* *Li*Polθ are more infective. (**A**) Coomassie blue stained SDS-PAGE gel of total extract from control *L. major* expressing endogenous Polθ, molecular marker, and varying amounts of total extract from pTEX-*Li*Polθ-transfected *L. major* overexpressing *Li*Polθ. Bottom, Western blot for *Li*Polθ using the *Li*Polθ antibody. (**B**) Growth curves of control (grey) and *Li*Polθ-overexpressing *L. major* (black). (**C**) Percentage of RAW cells infected with wild type control (grey bar), *Li*Polθ-overexpressing (black bar) and empty pTEX-transfected *L. major* (dashed bar) promastigotes.

tivity, and 5′ phosphate recognition in gaps, suggesting that unlike DNA polymerases from family X, *Li*Polθ does not function in classical NHEJ (43).

C. elegans Polθ was shown to perform single-patch BER in the absence of Polβ (44). In contrast, Polθ and Polβ were shown to synergistically contribute to BER in chicken DT40 cells (45). *Li*Polθ lacks dRP lyase activity, and therefore is not a good candidate for single-patch BER. It is worth noting that *Li*Polθ does not possess a helicase domain; however, a strong capacity for strand-displacement coupled to gap filling synthesis suggests potential roles in long-patch BER and alternative forms of NHEJ.

As described here, *Li*Polθ maintains Watson-Crick complementary nucleotide selection and is preferentially activated by Mn^{2+} ions. While replicative DNA polymerases use Mg^{2+} to maximize nucleotide insertion fidelity, other DNA polymerases take advantage of Mn^{2+} ions to maximize catalytic efficiency, with some reduction in fidelity (46–49). *Li*Polθ takes advantage of Mn^{2+} ion activation to tolerate various DNA lesions such as those induced by oxidative stress, e.g. 8oxodG, thymine glycol and abasic sites. *Li*Polθ 'reads' the 8oxodG by preferentially inserting dCTP (error-free) opposite the lesion. Moreover, *Li*Polθ extended 8oxodG:dCMP more efficiently than 8oxodG:dAMP, again favoring an error-free outcome during 8oxodG TLS. *Li*Polθ addresses abasic site and thymine glycol lesions by direct extension preferentially using dATP; however, these repairs would require another DNA polymerase for continued synthesis. Moreover, *Li*Polθ can accept distortions and looped-out bases, skipping unreadable lesions such as thymine glycol and abasic sites; this activity leads to the deletion of 1 nt. Similarly, human Polθ is also competent in TLS of thymine glycol or abasic sites (13).

Previous *in vivo* studies demonstrated that DT40 cells lacking Polθ were hypersensitive to H_2O_2 (45); this result is compatible with a role in either oxidative damage repair or tolerance and is in agreement with the data presented here that indicate that *Li*Polθ-overexpressing *Leishmania* are hyper-resistant to H_2O_2 (Table 1). Other *in vivo* studies in *D. melanogaster* (11,12) and *C. elegans* (50) have suggested a role for Polθ in interstrand crosslink repair. Again, *Li*Polθ-overexpression in *Leishmania* resulted in increased resistance to cisplatin- and mitomycin C-induced interstrand crosslinks (Table 1).

*Li*Polθ is primarily localized in the protozoa nucleus, and has a limited presence in the kinetoplast (Figure 7). This subcellular localization contrasts with the exclusive mitochondrial localization of Polγ, and with the preferential kinetoplast localization of the four trypanosomatid PolI-like family A DNA polymerases (26).

In conclusion, the *in silico*, *in vitro* and *in vivo* data, together with nuclear *Li*Polθ localization argue that *Li*Polθ is a true Polθ orthologue. *Li*Polθ is a proficient translesion synthesis DNA polymerase that can deal with several types of DNA damage. *In vivo* analysis demonstrated *Li*Polθ-dependent parasite resistance to genotoxicants and macrophage infectivity, strongly suggesting that *Li*Polθ has an important role in infection, most likely acting to protect the parasite from the intracellular oxidative damage that is characteristic of the macrophage host cell.

SUPPLEMENTARY DATA

Supplementary Data are available at NAR Online.

FUNDING

Spanish Ministry of Science and Innovation [AGL2010-21806-C02-01 to V.L., BFU2012-37969 to L.B.]; Comunidad de Madrid [S2010/BMD-2361 to L.B.]; Ramón Areces Foundation [050204100014 to V.L.]; Spanish Ministry of Science and Innovation fellowship (to A.F.O.). Funding for open access charge: Spanish Research Council, Spanish Ministry of Science and Innovation.
Conflict of interest statement. None declared.

REFERENCES

1. Singh,N., Kumar,M. and Singh,R. (2012) Leishmaniasis: current status of available drugs and new potential drug targets. *Asian Pacific J. Trop. Med.*, **5**, 485–497
2. W.H.O.2013. Leishmaniasis. *Fact sheet* 375
3. Desjeux,P. (2004) Leishmaniasis: current situation and new perspectives. *Comp. Immunol. Microbiol. Infect. Dis.*, **27**, 305–318.
4. W.H.O. Technical Report Series (2010) Control of the leishmaniasis. *W.H.O. anual report*. **949**, 1–201.
5. Cunningham,A.C. (2002) Parasitic adaptive mechanisms in infection by *Leishmania*. *Exp. Mol. Pathol.*, **72**, 132–141.
6. Sacks,D.L. and Perkins,P.V. (1984) Identification of an infective stage of *Leishmania* promastigotes. *Science*, **223**, 1417–1419.
7. Chang,K.P. and Dwyer,D.M. (1976) Multiplication of a human parasite (*Leishmania donovani)* in phagolysosomes of hamster macrophages *in vitro*. *Science*, **193**, 678–680.
8. Alexander,J. and Russell,D.G. (1992) The interaction of *Leishmania* species with macrophages. *Adv. Parasitol.*, **31**, 175–254.
9. Myler,P. and Fasel,N. (2008) *After the Genome*. Caister Academic Press, Norfolk.
10. Alcolea,P.J., Alonso,A., Sanchez-Gorostiaga,A., Moreno-Paz,M., Gomez,M.J., Ramos,I., Parro,V. and Larraga,V. (2009) Genome-wide analysis reveals increased levels of transcripts related with infectivity in peanut lectin non-agglutinated promastigotes of *Leishmania infantum*. *Genomics*, **93**, 551–564.
11. Boyd,J.B., Sakaguchi,K. and Harris,P.V. (1990) mus308 mutants of *Drosophila* exhibit hypersensitivity to DNA cross-linking agents and are defective in a deoxyribonuclease. *Genetics*, **125**, 813–819.
12. Harris,P.V., Mazina,O.M., Leonhardt,E.A., Case,R.B., Boyd,J.B. and Burtis,K.C. (1996) Molecular cloning of *Drosophila* mus308, a gene involved in DNA cross-link repair with homology to prokaryotic DNA polymerase I genes. *Mol. Cell. Biol.*, **16**, 5764–5771.
13. Seki,M., Masutani,C., Yang,L.W., Schuffert,A., Iwai,S., Bahar,I. and Wood,R.D. (2004) High-efficiency bypass of DNA damage by human DNA polymerase Q. *EMBO J.*, **23**, 4484–4494.
14. Yousefzadeh,M.J. and Wood,R.D. (2013) DNA polymerase POLQ and cellular defense against DNA damage. *DNA Repair (Amst.)*, **12**, 1–9.
15. Fernandez-Vidal,A., Guitton-Sert,L., Cadoret,J.C., Drac,M., Schwob,E., Baldacci,G., Cazaux,C. and Hoffmann,J.S. (2014) A role for DNA polymerase theta in the timing of DNA replication. *Nat. Commun.*, **5**, 4285.
16. Yousefzadeh,M.J., Wyatt,D.W., Takata,K., Mu,Y., Hensley,S.C., Tomida,J., Bylund,G.O., Doublie,S., Johansson,E., Ramsden,D.A., Mc Bride,K.M. and Wood,R.D. (2014) Mechanism of suppression of chromosomal instability by DNA polymerase POLQ. *PLoS Genet.*, **10**, e1004654.
17. Johnson,M., Zaretskaya,I., Raytselis,Y., Merezhuk,Y., McGinnis,S. and Madden,T.L. (2008) NCBI BLAST: a better web interface. *Nucleic Acids Res.*, **36**, W5–W9.
18. Papadopoulos,J.S. and Agarwala,R. (2007) COBALT: constraint-based alignment tool for multiple protein sequences. *Bioinformatics*, **23**, 1073–1079.
19. Sievers,F., Wilm,A., Dineen,D., Gibson,T.J., Karplus,K., Li,W., Higgins,D.G. *et al.* (2011) Fast, scalable generation of high-quality protein multiple sequence alignments using Clustal Omega. *Mol. Syst. Biol.*, **7**, 539.
20. Kelly,J.M., Ward,H.M., Miles,M.A. and Kendall,G. (1992) A shuttle vector which facilitates the expression of transfected genes in *Trypanosomacruzi* and *Leishmania*. *Nucleic Acids Res.*, **20**, 3963–3969.
21. Robinson,K.A. and Beverley,S.M. (2003) Improvements in transfection efficiency and tests of RNA interference (RNAi) approaches in the protozoan parasite *Leishmania*. *Mol. Biochem. Parasitol.*, **128**, 217–228.
22. Kornberg,A. and Baker,T. (1992) *DNA Replication*. Freeman, NY.
23. Graziewicz,M.A., Longley,M.J. and Copeland,W.C. (2006) DNA polymerase gamma in mitochondrial DNA replication and repair. *Chem. Rev.*, **106**, 383–405.
24. Takata,K., Shimizu,T., Iwai,S. and Wood,R.D. (2006) Human DNA polymerase N (POLN) is a low fidelity enzyme capable of error-free bypass of 5S-thymine glicol. *J. Biol. Chem.*, **281**, 23445–23455.
25. Bernad,A., Blanco,L., Lazaro,J.M., Martin,G. and Salas,M. (1989) A conserved 3'—-5' exonuclease active site in prokaryotic and eukaryotic DNA polymerases. *Cell*, **59**, 219–228.
26. Klingbeil,M.M., Motyka,S.A. and Englund,P.T. (2002) Multiple mitochondrial DNA polymerases in *Trypanosoma brucei*. *Mol. Cell*, **10**, 175–186.
27. Bruhn,D.F., Mozeleski,B., Falkin,L. and Klingbeil,M.M. (2010) Mitochondrial DNA polymerase POLIB is essential for minicircle DNA replication in African trypanosomes. *Mol. Microbiol.*, **75**, 1414–1425.
28. Bruhn,D.F., Sammartino,M.P. and Klingbeil,M.M. (2011) Three mitochondrial DNA polymerases are essential for kinetoplast DNA replication and survival of bloodstream form *Trypanosoma brucei*. *Eukaryot. Cell*, **10**, 734–743.
29. Hogg,M., Seki,M., Wood,R.D., Doublie,S. and Wallace,S.S. (2011) Lesion bypass activity of DNA polymerase theta (POLQ) is an intrinsic property of the pol domain and depends on unique sequence inserts. *J. Mol. Biol.*, **405**, 642–652.
30. Taladriz,S., Hanke,T., Ramiro,M.J., Garcia-Diaz,M., Garcia De Lacoba,M., Blanco,L. and Larraga,V. (2001) Nuclear DNA polymerase beta from *Leishmania infantum*. Cloning, molecular analysis and developmental regulation. *Nucleic Acids Res.*, **29**, 3822–3834.
31. Garcia-Diaz,M., Bebenek,K., Sabariegos,R., Dominguez,O., Rodriguez,J., Kirchhoff,T., Garcia-Palomero,E., Picher,A.J., Juarez,R., Ruiz,J.F., Kunkel,T.A. and Blanco,L. (2002) DNA polymerase lambda, a novel DNA repair enzyme in human cells. *J. Biol. Chem.*, **277**, 13184–13191.
32. Alonso,A., Terrados,G., Picher,A.J., Giraldo,R., Blanco,L. and Larraga,V. (2006) An intrinsic 5'-deoxyribose-5-phosphate lyase activity in DNA polymerase beta from *Leishmania infantum* supports a role in DNA repair. *DNA Repair (Amst.)*, **5**, 89–101
33. Dogliotti,E., Fortini,P., Pascucci,B. and Parlanti,E. (2001) The mechanism of switching among multiple BER pathways. *Prog Nucleic Acids Res. Mol. Biol.*, **68**, 3–27.
34. Mateos-Gomez,P.A., Gong,F., Nair,N., Miller,K.M., Lazzerini-Denchi,E. and Sfeir,A. (2015) Mammalian polymerase theta promotes alternative NHEJ and suppresses recombination. *Nature*, **518**, 254–257.
35. Kent,T., Chandramouly,G., McDevitt,S.M., Ozdemir,A.Y. and Pomerantz,R.T. (2015) Mechanism of microhomology-mediated end-joining promoted by human DNA polymerase theta. *Nat. Struct. Mol. Biol.*, **22**, 230–237.
36. Batra,V.K., Beard,W.A., Hou,E.W., Pedersen,L.C., Prasad,R. and Wilson,S.H. (2010) Mutagenic conformation of 8-oxo-7,8-dihydro-2'-dGTP in the confines of a DNA polymerase active site. *Nat. Struct. Mol. Biol.*, **17**, 889–890.
37. Katafuchi,A. and Nohmi,T. (2010) DNA polymerases involved in the incorporation of oxidized nucleotides into DNA: their efficiency and template base preference. *Mutat. Res.*, **703**, 24–31.
38. Moriya,M. (1993) Single-stranded shuttle phagemid for mutagenesis studies in mammalian cells: 8-oxoguanine in DNA induces targeted G.C–>T.A transversions in simian kidney cells. *Proc. Natl. Acad. Sci. U.S.A.*, **90**, 1122–1126.
39. Yoon,J.H., Bhatia,G., Prakash,S. and Prakash,L. (2010) Error-free replicative bypass of thymine glycol by the combined action of DNA polymerases kappa and zeta in human cells. *Proc. Natl. Acad. Sci. U.S.A.*, **107**, 14116–14121.

40. Yoon,J.H., Roy Choudhury,J., Park,J., Prakash,S. and Prakash,L. (2014) A role for DNA polymerase theta in promoting replication through oxidative DNA lesion, thymine glycol, in human cells. *J. Biol. Chem.*, **289**, 13177–13185.
41. Lindahl,T. (1993) Instability and decay of the primary structure of DNA. *Nature*, **362**, 709–715
42. Avkin,S., Adar,S., Blander,G. and Livneh,Z. (2002) Quantitative measurement of translesion replication in human cells: evidence for bypass of abasic sites by a replicative DNA polymerase. *Proc. Natl. Acad. Sci. U.S.A.*, **99**, 3764–3769.
43. Martin,M.J. and Blanco,L. (2012) Evolving DNA repair polymerases: from double-strand break repair to base excision repair and VDJ recombination. In: *DNA Repair – New Research Directions*. pp. 85–121.
44. Asagoshi,K., Lehmann,W., Braithwaite,E.K., Santana-Santos,L., Prasad,R., Freedman,J.H., Van Houten,B. and Wilson,S.H. (2012) Single-nucleotide base excision repair DNA polymerase activity in *C. elegans* in the absence of DNA polymerase beta. *Nucleic Acids Res.*, **40**, 670–681.
45. Yoshimura,M., Kohzaki,M., Nakamura,J., Asagoshi,K., Sonoda,E., Hou,E., Prasad,R., Wilson,S.H., Tano,K., Yasui,A. *et al.* (2006) Vertebrate POLQ and POLbeta cooperate in base excision repair of oxidative DNA damage. *Mol. Cell*, **24**, 115–125.
45. Blanca,G., Shevelev,I., Ramadan,K., Villani,G., Spadari,S., Hubscher,U. and Maga,G. (2003) Human DNA polymerase lambda diverged in evolution from DNA polymerase beta toward specific Mn(++) dependence: a kinetic and thermodynamic study. *Biochemistry*, **42**, 7467–7476.
47. Frank,E.G. and Woodgate,R. (2007) Increased catalytic activity and altered fidelity of human DNA polymerase iota in the presence of manganese. *J. Biol. Chem.*, **282**, 24689–24696.
48. Sanchez-Berrondo,J., Mesa,P., Ibarra,A., Martinez-Jimenez,M.I., Blanco,L., Mendez,J., Boskovic,J. and Montoya,G. (2012) Molecular architecture of a multifunctional MCM complex. *Nucleic Acids Res*, **40**, 1366–1380.
49. Martinez-Jimenez,M.I., Garcia-Gomez,S., Bebenek,K., Sastre-Moreno,G., Calvo,P.A., Diaz-Talavera,A., Kunkel,T.A. and Blanco,L. (2015) Alternative solutions and new scenarios for translesion DNA synthesis by human PrimPol. *DNA Repair (Amst.)*, **29**, 127–138.
50. Muzzini,D.M., Plevani,P., Boulton,S.J., Cassata,G. and Marini,F. (2008) *Caenorhabditis elegans* POLQ-1 and HEL-308 function in two distinct DNA interstrand cross-link repair pathways. *DNA Repair (Amst.)*, **7**, 941–950.